

2

WRDC-TR-89-2083



CAPILLARY FLOW PROPERTIES OF MESH WICKS

Jay H. Ambrose
Louis C. Chow

University of Kentucky
Department of Mechanical Engineering
Lexington, KY 40506-0046

July 1989

Interim Report for Period July 1987 - August 1988

Approved for public release; distribution unlimited.

DTIC
ELECTE
NOV 29 1989
S E D

AERO PROPULSION & POWER LABORATORY
WRIGHT RESEARCH & DEVELOPMENT CENTER
AIR FORCE SYSTEMS COMMAND
WRIGHT-PATTERSON AIR FORCE BASE, OHIO 45433-6563

AD-A214 769

NOTICE

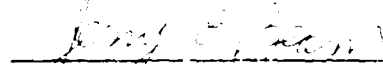
When Government drawings, specifications, or other data are used for any purpose other than in connection with a definitely Government-related procurement, the United States Government incurs no responsibility or any obligation whatsoever. The fact that the government may have formulated or in any way supplied the said drawings, specifications, or other data, is not to be regarded by implication, or otherwise in any manner construed, as licensing the holder, or any other person or corporation; or as conveying any rights or permission to manufacture, use, or sell any patented invention that may in any way be related thereto.

This report is releasable to the National Technical Information Service (NTIS). At NTIS, it will be available to the general public, including foreign nations.

This technical report has been reviewed and is approved for publication.

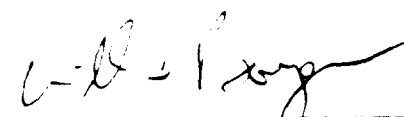


MICHAEL J. MORGAN
Power Technology Branch
Aerospace Power Division
Aero Propulsion and Power Laboratory



JERRY E. BEAM
Power Technology Branch
Aerospace Power Division
Aero Propulsion and Power Laboratory

FOR THE COMMANDER



WILLIAM U. BORGER
Chief, Aerospace Power Division
Aero Propulsion & Power Laboratory

If your address has changed, if you wish to be removed from our mailing list, or if the addressee is no longer employed by your organization please notify WRDC/PO5, WPAFB, OH 45433-6563 to help us maintain a current mailing list.

Copies of this report should not be returned unless return is required by security considerations, contractual obligations, or notice on a specific document.

REPORT DOCUMENTATION PAGE				Form Approved OMB No 0704-0188	
1a REPORT SECURITY CLASSIFICATION Unclassified			1b RESTRICTIVE MARKINGS		
2a SECURITY CLASSIFICATION AUTHORITY			3 DISTRIBUTION/AVAILABILITY OF REPORT Approved for public release, Distribution is unlimited.		
2b DECLASSIFICATION/DOWNGRADING SCHEDULE					
4 PERFORMING ORGANIZATION REPORT NUMBER(S) UK-ME-88-08			5 MONITORING ORGANIZATION REPORT NUMBER(S) WRDC-TR-89-2083		
6a NAME OF PERFORMING ORGANIZATION University of Kentucky		6b OFFICE SYMBOL (If applicable)		7a NAME OF MONITORING ORGANIZATION Aero Propulsion and Power Laboratory (WRDC/POOS) Wright Research and Development Center, AFSC	
6c ADDRESS (City, State, and ZIP Code) Department of Mechanical Engineering Lexington, KY 40506-0046			7b ADDRESS (City, State, and ZIP Code) Wright-Patterson AFB, OH 45433-6563		
8a NAME OF FUNDING/SPONSORING ORGANIZATION		8b OFFICE SYMBOL (If applicable)		9 PROCUREMENT INSTRUMENT IDENTIFICATION NUMBER F33615-87-C-2777	
8c ADDRESS (City, State, and ZIP Code)			10 SOURCE OF FUNDING NUMBERS		
			PROGRAM ELEMENT NO. 63221C	PROJECT NO. 0812	TASK NO. 00
11 TITLE (Include Security Classification) Capillary Flow Properties of Mesh Wicks					
12 PERSONAL AUTHOR(S) Ambrose, Jay H.; Chow, Louis C.					
13a TYPE OF REPORT Interim		13b TIME COVERED FROM 87 JUL TO 88 AUG		14 DATE OF REPORT (Year, Month, Day) July 1989	
15 PAGE COUNT 44					
16 SUPPLEMENTARY NOTATION					
17 COSATI CODES			18 SUBJECT TERMS (Continue on reverse if necessary and identify by block number) Capillary pressure, mesh wick, porous medium, saturation, permeability		
FIELD	GROUP	SUB-GROUP			
19 ABSTRACT (Continue on reverse if necessary and identify by block number) The objective of the present investigation is to measure the saturation dependence of the capillary flow properties for multilayer, square mesh screen wicks. X-ray radiography is used to measure the saturation in the wicks. Results are presented for the capillary pressure and saturation relationship from steady-state tests. The capillary pressure curves are shown to correlate well when cast in terms of the dimensionless Leverett function. Results of transient wicking rise tests are also presented. The transient saturation distributions are used to calculate the relative permeability of the partially saturated wick structures.					
20 DISTRIBUTION/AVAILABILITY OF ABSTRACT <input checked="" type="checkbox"/> UNCLASSIFIED/UNLIMITED <input type="checkbox"/> SAME AS RPT <input type="checkbox"/> DTIC USERS				21 ABSTRACT SECURITY CLASSIFICATION Unclassified	
22a NAME OF RESPONSIBLE INDIVIDUAL Dr. Jerry E. Beam				22b TELEPHONE (Include Area Code) (513)255-6241	
				22c OFFICE SYMBOL WRDC/POOS	

FOREWORD

The research reported is part of a continuing investigation of transient heat pipe response. The research is sponsored by the Air Force Aero Propulsion and Power Laboratory, Wright Research and Development Center. Dr. Jerry E. Beam of the Nuclear/Thermal Technology Group is the technical contract monitor during the reporting period.

The research was conducted primarily in the Heat Transfer and Phase Change Laboratory at the University of Kentucky. The technical assistance provided by Drs. Tom Mahaffey and Wei Soon Chang is appreciated.

Accession For	
NTIS GRA&I	<input checked="" type="checkbox"/>
DTIC TAB	<input type="checkbox"/>
Unannounced	<input type="checkbox"/>
Justification	
By	
Distribution/	
Availability Codes	
Dist	Avail and/or Special
A-1	



TABLE OF CONTENTS

SECTION	PAGE
I. INTRODUCTION	1
II. OBJECTIVE OF THE RESEARCH EFFORT	2
III. BACKGROUND	3
IV. MEASUREMENT OF SATURATION USING X RAYS	5
4.1 Selection of X-Ray Equipment	5
4.2 X-Ray Radiography System	6
4.3 X-Ray Film Digitizing System	9
4.4 Heat Pipe Fill Station	9
V. SATURATION DEPENDENCE OF CAPILLARY PRESSURE	13
5.1 Theory of Capillary Pressure	13
5.2 Screen Wicks	13
5.3 Steady-State Tests	14
5.4 Transient Tests	16
5.5 Dimensionless Capillary Pressure	22
5.6 Graphite Wick Material	25
VI DETERMINATION OF RELATIVE PERMEABILITY	27
6.1 Theory of Relative Permeability	27
6.2 Determination of Relative Permeability from Transient Wicking Tests	27
6.3 Relative Permeability Experiments	30
6.4 Preliminary Results	32
VII. CONCLUSIONS AND RECOMMENDATIONS	34
REFERENCES	35

LIST OF ILLUSTRATIONS

FIGURE		PAGE
1	X-Ray System for Saturation Measurement	7
2	X-Ray Beam Shutter System	8
3	X-Ray Film Digitizing System	10
4	Heat Pipe Fill Station	11
5	Steady-State Wicking Apparatus	15
6	Transient Wicking Rise in HC7-85 Wick	17
7	Transient Saturation Distribution, 5-280 Wick	18
8	Transient Saturation Distribution, HC7-200 Wick	19
9	Transient Saturation Distribution, HC7-85 Wick	20
10	Transient Saturation Distribution, HC7-51 Wick	21
11	Dimensionless Capillary Pressure vs Saturation	23
12	Leverett Function	24
13	Leverett Function with Graphite Wick	26
14	Relative Permeability vs Saturation	29
15	New Apparatus for Measuring Relative Permeability	31

LIST OF TABLES

TABLE		PAGE
1	Wick Material Properties	14

I. INTRODUCTION

Prediction of transient heat pipe behavior is extremely important in the design of thermal control systems for all types of spacecraft. Heat pipes are an important element in spacecraft thermal control. Heat pipes may be subjected to pulsed-heat loading or rapid transients. Previous work in this area has pointed out the need for detailed modeling of the liquid flow in the wick. The amount of liquid in any portion of the wick depends not only on the instantaneous heat input and rejection, but on the loading history.

Development of a detailed liquid flow model depends upon knowledge of the saturation dependence of the flow properties, because the detailed flow model accounts for the variation in saturation in the wick with position and time.

This report describes a research effort to determine the saturation dependence of the flow properties in a heat pipe wick. The report is divided into three sections covering the x-ray saturation measurement system, the measurement of capillary pressure and the measurement of relative permeability.

II. OBJECTIVE OF THE RESEARCH EFFORT

The objective of the research effort is to study the liquid flow in mesh and groove wicks and to develop a detailed model of the liquid flow which includes saturation dependence of the important flow parameters.

III. BACKGROUND

The flow of fluids in capillary structures has been studied extensively in the past, especially in connection with geological flows. The flow of fluids in porous wick materials has become an important subject because of numerous modern heat transfer applications such as heat pipes and enhanced boiling surfaces. Modeling of fluid flow in porous materials requires knowledge of two major flow properties, namely capillary pressure P_c , and permeability K . These two properties depend on the amount of liquid filling the voids of the porous structure, characterized by the saturation S . Saturation is defined as the ratio of liquid volume to the void volume. For a fully saturated wick structure ($S=1$), a full permeability K is used. The variation in permeability for a partially saturated wick structure is accounted for by multiplying K by the relative permeability $K_r(S)$, with $0 < K_r < 1$.

Although much information has been published on the flow properties of wick materials, relatively little information can be found regarding the saturation dependence of P_c and K_r . The accuracy of fluid flow models for wick structures is limited by this fact, especially if significant saturation gradients or transient saturation distributions occur. Fluid flows in wick structures are generally modeled by assuming a fully saturated structure (constant properties).

Extensive modeling of heat transfer and fluid flow in partially saturated packed beds of sand has been carried out by Udell and coworkers [1-3], including the effect of saturation gradients on the capillary pressure and relative permeabilities. Available data for the sand/water system were utilized to model these effects. In particular, the researchers used a correlation of the data of Leverett [4] for the dimensionless capillary pressure, and the following relative permeability expressions for the liquid and vapor phases, respectively:

$$\begin{aligned} K_{rl} &= s \\ K_{rv} &= (1-s)^3 \end{aligned}$$

where

$$s = \frac{(S-S_i)}{(1-S_i)}$$

and S_i is the "immobile saturation." The third power saturation dependence of the relative permeability to the liquid phase has been shown to agree with experimental data for granular porous media [5].

Initial results have been previously presented [6] for the static wicking rise test. Also presented were results for mass flow rate and saturation gradient in a wick structure heated at one end. The ratio of superficial velocity and saturation gradient was used to determine the saturation dependence of a "liquid diffusivity," which includes effects of both capillary pressure and relative permeability. However, because capillary pressure depends on saturation, surface tension, contact angle and wick geometry while relative permeability depends predominantly on saturation and wick geometry alone, it is desirable to separate the two flow properties and study them separately.

IV. MEASUREMENT OF SATURATION USING X RAYS

Development of the liquid flow model relies on measurements of saturation distributions in heat pipe wicks. We have used x-ray radiography for saturation measurements in heat pipe wicks under various operating conditions. Preliminary investigation using this method utilized the x-ray facility located at the Air Force Materials Laboratory. It was desirable to develop a system which could be dedicated full time to this effort, and which was more suitable for the low-energy radiography used for imaging liquids. For these reasons, a facility has been developed at UK specifically for measurement of saturation in heat pipe wicks. This section describes the various components which include an x-ray tube and power supply, radiation shielded chamber, x-ray shutter system and x-ray film digitizing system. A heat pipe fill station was also fabricated for filling the beryllium wall heat pipe.

4.1 SELECTION OF X-RAY EQUIPMENT

Several experiments involving saturation measurements were performed using x-ray equipment located at the Air Force Materials Laboratory. From these experiments the energy requirements of the x-ray source have been well defined. All of the previous work has been accomplished with x rays produced at an operating tube voltage of 12 to 25 kV. This energy level is well below the rated limits of the various machines which were available at the Materials Laboratory. An x-ray source better suited to these low-energy levels has been purchased. The Kevex model K3052S x-ray tube operates at 5 to 30-kV and 0 to 6.7 mA tube current and hence is ideal for low-energy x-ray imaging.

During evaluation of the various options for x-ray systems, a real-time x-ray imaging system was also evaluated. There are many advantages to the use of real-time x-ray imaging instead of conventional x-ray radiography. Because the image may be digitized and stored using a digital video device, the saturation measurements are not only continuous in time but position also. The tedious process of scanning radiographs with a photodensitometer would be unnecessary.

The disadvantages to using real-time x-ray imaging are loss of resolution and cost. The loss of resolution was not considered to be of major importance to the present study because resolution of fine details is unnecessary.

However, cost proved to be a deciding factor. A real-time system uses an image intensifier which is quite expensive (\$10,000-\$20,000). In addition, the intensifier will not operate effectively at x-ray energies below 30 kV. This put the system at the upper limit of the useful range of energies for the present study. In all, the real-time system would cost at least twice as much as the conventional system. Because the proposed work involves a good deal of steady-state measurements, the additional expense of the real-time system could not be justified.

Transient measurements are obtained using conventional radiography by taking multiple exposures at very low exposure times. Good results have been obtained with exposure times as low as 1 second using direct exposure film.

4.2 X-RAY RADIOGRAPHY SYSTEM

Before receiving the x-ray tube and power supply from Kevex, a lead-lined chamber was fabricated. This was necessary so that the x-ray tube can be operated in the existing laboratory room without subjecting workers to unsafe radiation levels. The chamber is shown in the diagram in Figure 1. It consists of a steel chamber with a single latched door and a secure feedthrough. Safety measures include approximately 1 mm of lead shielding over the entire exterior, a safety interlock on the chamber door and a red warning beacon on the top of the chamber. Two positions for the x-ray tube have been used, to provide either a horizontal or vertical beam. A lead shutter system is employed to provide very accurate control of the exposure time and remove the effects of power rampup associated with the power supply. Once the x-ray source has been activated, the power source takes anywhere from 10 to 40 seconds to reach the set power level depending on power level. Since the exposure times are sometimes of the order of seconds, to achieve accurate exposure times the x-ray tube should be operating at the desired power level at the start of the exposure period. Details of the shutter system are shown in Figure 2. The two lead shutters are driven by a stepping motor, which is controlled by a computer. Exposure time is set using computer's onboard clock. For each exposure the x-ray tube is allowed to operate at the desired constant power level and then the shutter is activated by a remote switch.

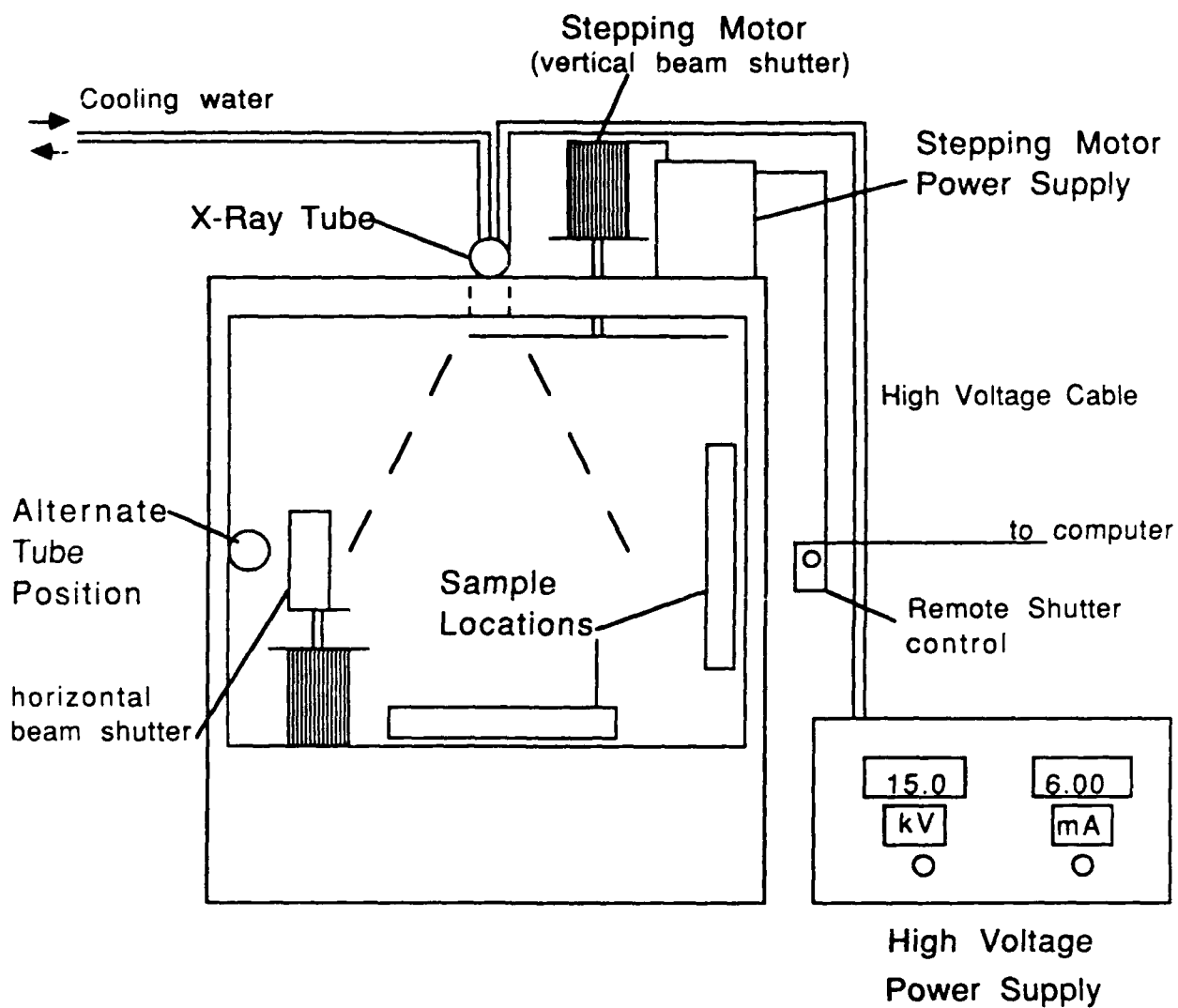
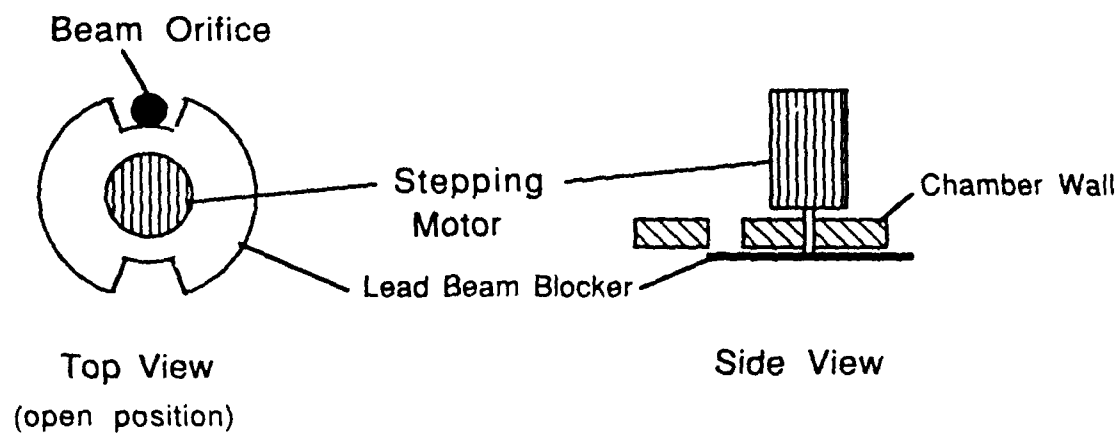
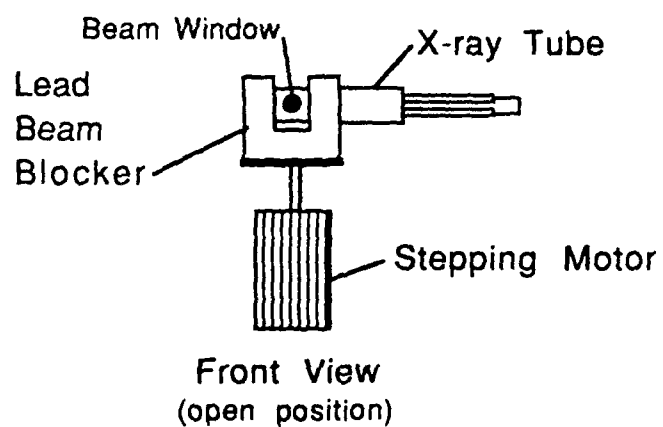


Figure 1 X-Ray System for Saturation Measurement



Vertical Beam Shutter



Horizontal Beam Shutter

Figure 2 X-Ray Beam Shutter System

4.3. X-RAY FILM DIGITIZING SYSTEM

Previous saturation values were obtained using either an automatic recording microphotodensitometer located at Wright-Patterson Materials Laboratory or a manual photodensitometer at the University of Kentucky. Because it is desirable to obtain optical density values for as many locations as possible on each of many films, partial automation of the system was deemed necessary. The photodensitometer at UK was already equipped with a RS232 communications port option. An x-y positioner for the film was fabricated to be used with the photodensitometer. The x-axis motion of the positioner is controlled by a stepping motor, which is driven by a data acquisition and control board on a personal computer. A schematic of the system is shown in Figure 3. Since the size of the films is always 12 by 1 in., the one axis automation is sufficient. The computer program positions the film along the x-axis, reads the optical density from the photodensitometer and then repeats with a variable distance increment. After a complete scan along the 12-in. length of the x-direction, the manual y-direction positioning mechanism is advanced one increment, and the scan is repeated. An average scan consists of a 0.1-in. by 0.1-in. grid and approximately 150 readings per 3-in. section of film.

4.4 HEAT PIPE FILL STATION

A simple heat pipe fill station has been fabricated and installed to evacuate and charge the beryllium heat pipe. It will also be used later to fill the heat pipes used to demonstrate TES pulse mitigation techniques. The heat pipe fill station is shown in Figure 4. It is constructed of glass. A two-stage mechanical pump is used to evacuate the system. In order to reduce noncondensable gas concentration, a flushing procedure will be used. A LN_2 cold trap has been included for removing the working fluid inventory during the flushing procedure. The flushing procedure allows reduction of noncondensable gas (NCG) concentrations to approximately the same level as if the heat pipe were evacuated to 10^{-6} torr. For example, consider the heat pipe is initially evacuated to 10^{-6} torr. Assuming that only NCG remains in the pipe, its partial pressure P_g is also 10^{-6} torr. If the pipe is then

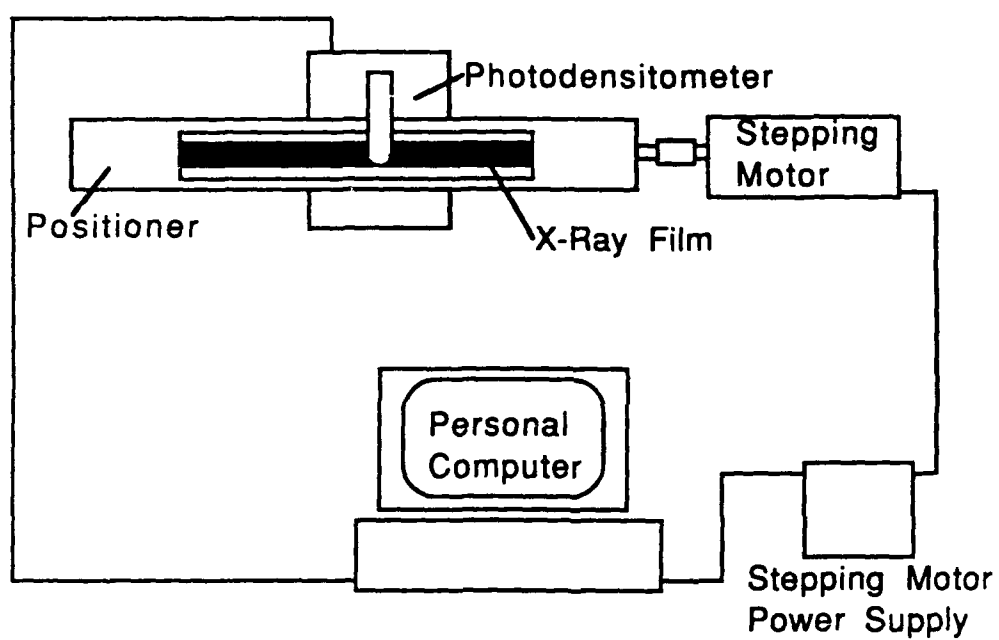


Figure 3 X-Ray Film Digitizing System

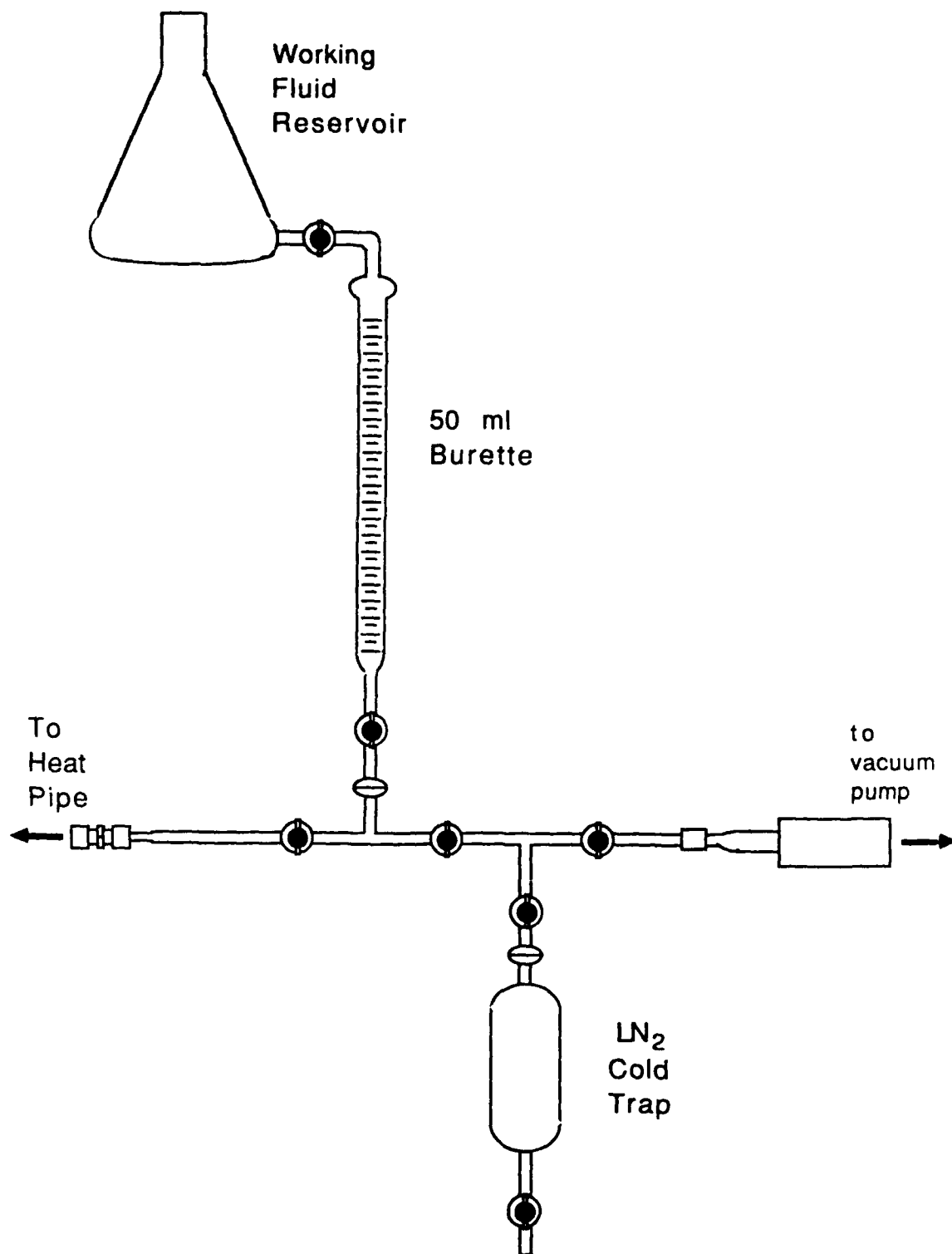


Figure 4 Heat Pipe Fill Station

backfilled with Freon-113 at room temperature, the concentration of NCG is $P_g/P_{tot} = 3.6 \times 10^{-9}$. If instead the pipe is evacuated to only 0.1 torr, the same NCG concentration can be achieved after two flushes. This involves three evacuations and fillings; the final fill is the prescribed charge.

V. SATURATION DEPENDENCE OF CAPILLARY PRESSURE

In the present investigation capillary pressure has been measured as a function of saturation in heat pipe wicks. Measurements of the capillary rise height in polyester mesh wicks were performed under transient and steady-state conditions. Under steady-state conditions, the capillary pressure is equal to the hydrostatic head. For transient conditions, the capillary pressure is different than the hydrostatic term.

5.1 THEORY OF CAPILLARY PRESSURE

The saturation dependence of the capillary pressure is complicated by hysteresis. The functional relationship depends upon whether the wetting phase is displacing the nonwetting phase (rising case) or being displaced by it (falling case). There exists in the falling case an irreducible or immobile saturation below which no liquid flow can take place. In this case, called the pendular regime, the discrete portions of the liquid phase can experience mass flow only through evaporation and condensation. This irreducible saturation is evident in the data of Leverett [4] for sands, but is absent from the data of Eninger [7] for a metal fiber wick. In the present report, data is presented for the rising case only. Complete data for the falling case have not been obtained as of the date of this report.

The capillary pressure may be measured under either the static (no flow of liquid) or dynamic conditions (liquid flow due to capillary pressure gradient). Brown [8] has shown the static and dynamic capillary pressure distributions measured in limestone cores to be identical. In the present work, it has been assumed that the relationship between capillary pressure and saturation for a given wick/fluid combination is a function of saturation alone.

5.2 SCREEN WICKS

The wick materials used were all square mesh synthetic fabrics manufactured by Tetko, Inc. Their relevant properties are given in Table 1.

Table 1. Wick Material Properties

Material Type	Mesh Number(in^{-1})	Filament Dia.(mil)	Single Layer Thickness (mil)	K ($\times 10^{-10}, \text{m}^2$)	ϵ
polypropylene 5-280	58.0	6.3	12.6	7.88	0.70
polyesters HC7-200	84.7	3.9	6.5	4.18	0.73
HC7-85	203.2	1.6	2.6	0.74	0.73
HC7-51	302.4	1.3	2.6	0.26	0.68

In both cases (transient and steady state), the wick structures were held between two flat beryllium plates. This was required to maintain the wicks in a planar geometry and ensure good contact between layers of wick material. This geometry is different than most heat transfer applications (e.g., heat pipes) where the wick is bounded on only one side by a solid surface. However, as will be discussed later, the boundary effects in the materials of interest are confined to such a thin region that effects on the flow properties can be safely assumed negligible.

The wicks were radiographed using the x-ray source with the tube voltage set at 15 kV. Average saturation distributions were obtained from optical density measurements taken on a 0.1-in. by 0.1-in. grid, and then averaged in the direction perpendicular to the pressure gradient.

5.3 STEADY-STATE TESTS

The steady-state wicking apparatus is shown in Figure 5. A closed system was utilized to minimize the effects of evaporation of the liquid on the final equilibrium distribution. The design is similar to that used by Shibayama and Morooka [9] with the addition of the saturation measurement. A metal marker was used to show, on the radiograph, the location of the free liquid interface in the glass tube. For each test, the wick was cleaned in acetone, rinsed with methanol filtered through a 0.2- μm filter and dried with filtered air. It was then assembled into the holder and the beryllium plates were sealed in place with silicone sealant.

The steady-state tests were to be performed with Freon-113 because of its superior x-ray attenuation property. However, Freon-113 was found to be

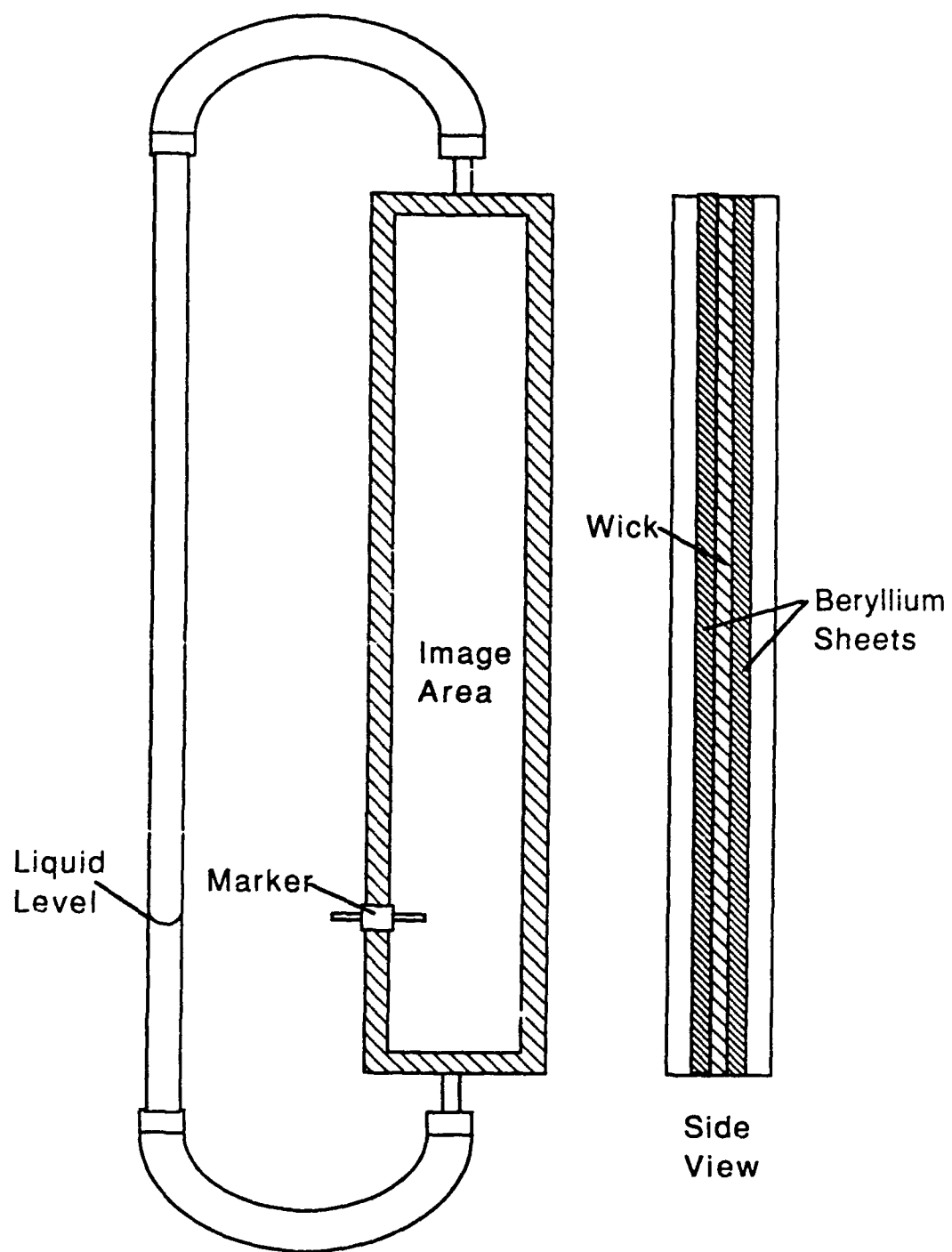


Figure 5 Steady-State Wicking Apparatus

incompatible with the sealant, so doped methanol was used in its place. The methanol was doped with a small amount (0.0375 g/ml) of potassium iodide to increase x-ray absorption. Rise tests were conducted in capillary tubes to verify that the small amount of impurity had a negligible effect on surface tension and contact angle.

A radiograph was taken of the assembly with a dry wick. Kodak Type M industrial radiography film was used for the steady-state tests. Liquid was added to the glass tube. More liquid was added as necessary to maintain the liquid level in the glass tube. Equilibrium was assumed to have been reached when the liquid level in the tube stopped falling, and another radiograph was taken to determine the rising saturation distribution. The levels in the tube were monitored at half hour intervals. Equilibrium was based on no perceptable change in liquid level during one interval. In all cases, the duration of the steady-state tests was of the order of 1 hour.

5.4 TRANSIENT TESTS

Transient wicking tests were conducted with an open system. Because of the much shorter duration of these tests (of the order of 1 minute), evaporation is assumed negligible. The wick layers were clamped between the two beryllium plates, with the sides open to the atmosphere. Each test consisted of placing the wick in contact with a constant head reservoir of liquid at time $t=0$. Freon-113 was used in the transient tests, because of its good x-ray attenuation. The saturation distributions were measured at intervals of 15 to 45 seconds with a 1-second exposure time. The short exposure times were made possible through use of high speed, Kodak direct exposure film. The image of a wicking front characteristic of these tests is shown in Figure 6. These prints are reproduced directly from the x-ray film. The flow in this case is a moving front characteristic of that which occurs when a previously dry wick structure is rewetted with liquid. After equilibrium has been established, the pressure gradient is hydrostatic, and the usual curve of static capillary pressure versus saturation may be obtained. Transient saturation distributions for the four wick materials in Table 1 are shown in Figures 7 to 10. The time values correspond to seconds elapsed since filling and distances are measured from the free liquid surface. These results are in qualitative agreement with measurements of Beam [10] for

Freon-113 in 203 square mesh polyester 15 layer wick.
Vertical wicking rise. Liquid introduced at time $t=0$.
Elapsed time in seconds.

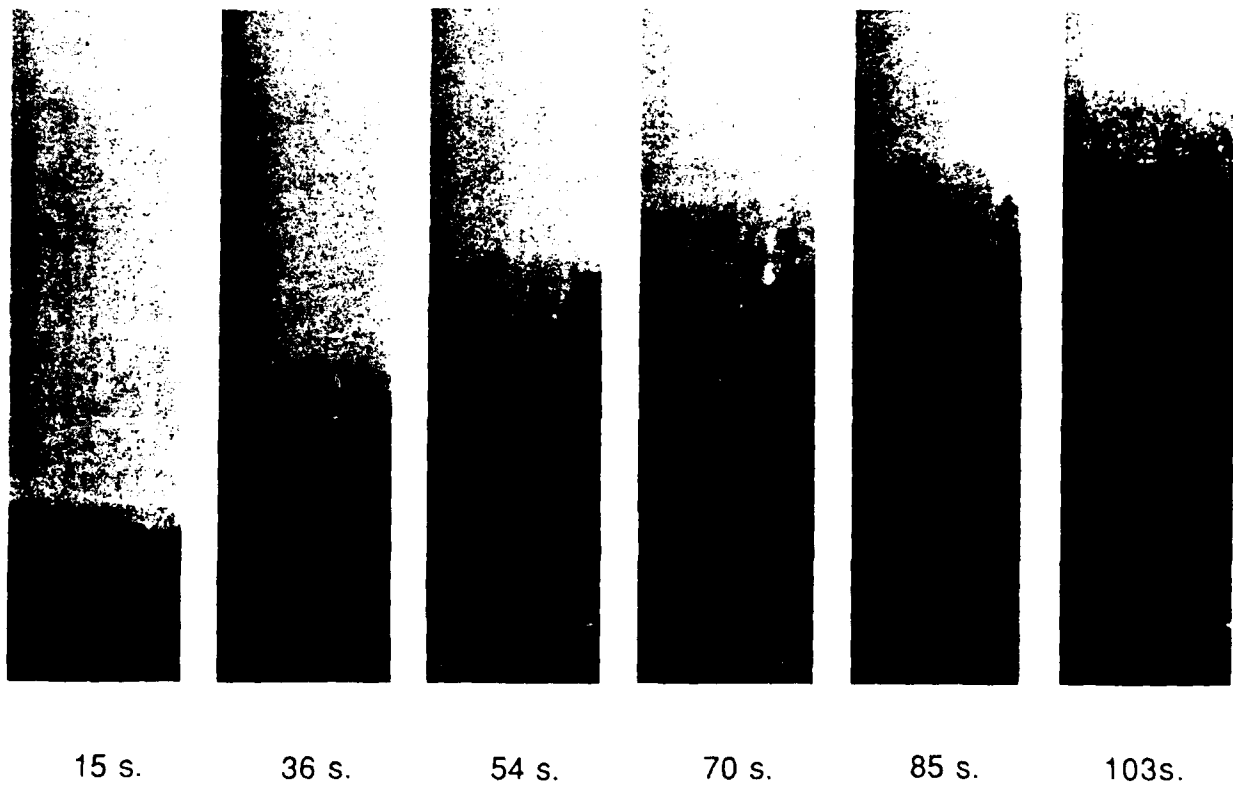


Figure 6 Transient Wicking Rise in HC7-85 Wick

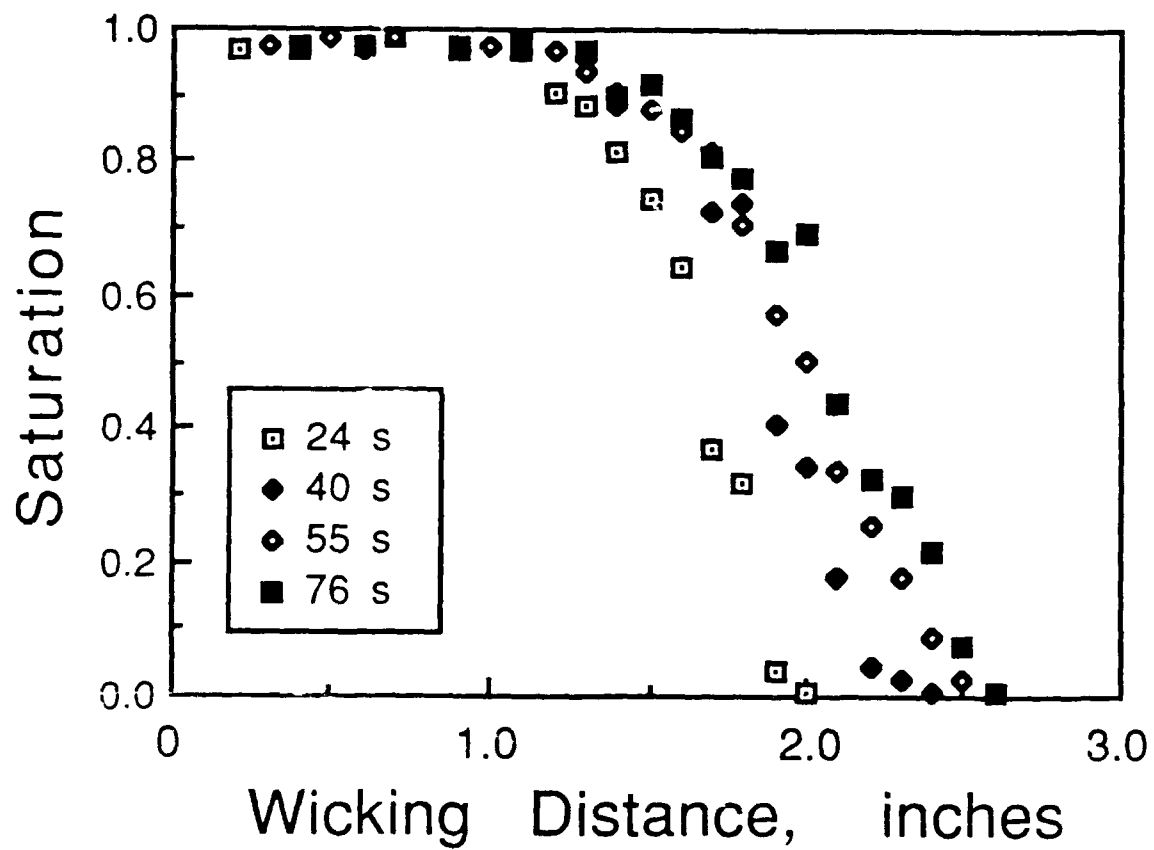


Figure 7 Transient Saturation Distribution, 5-280 Wick

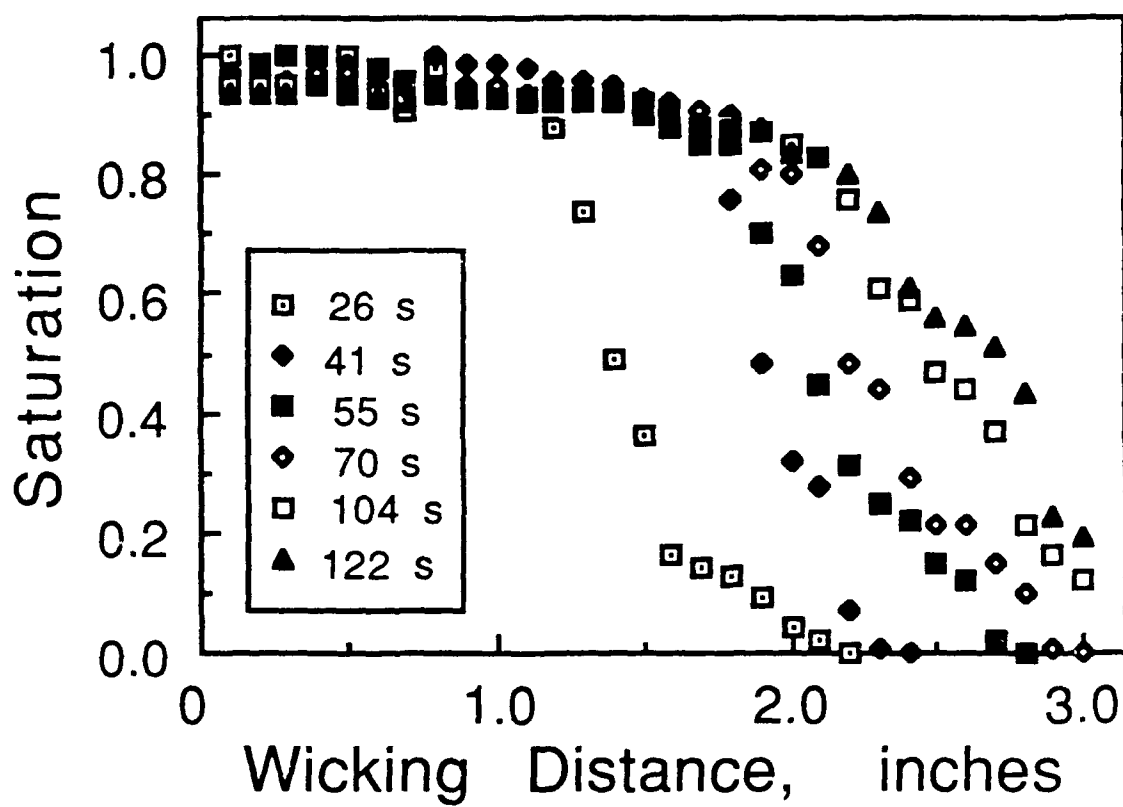


Figure 8 Transient Saturation Distribution, HC7-200 Wick

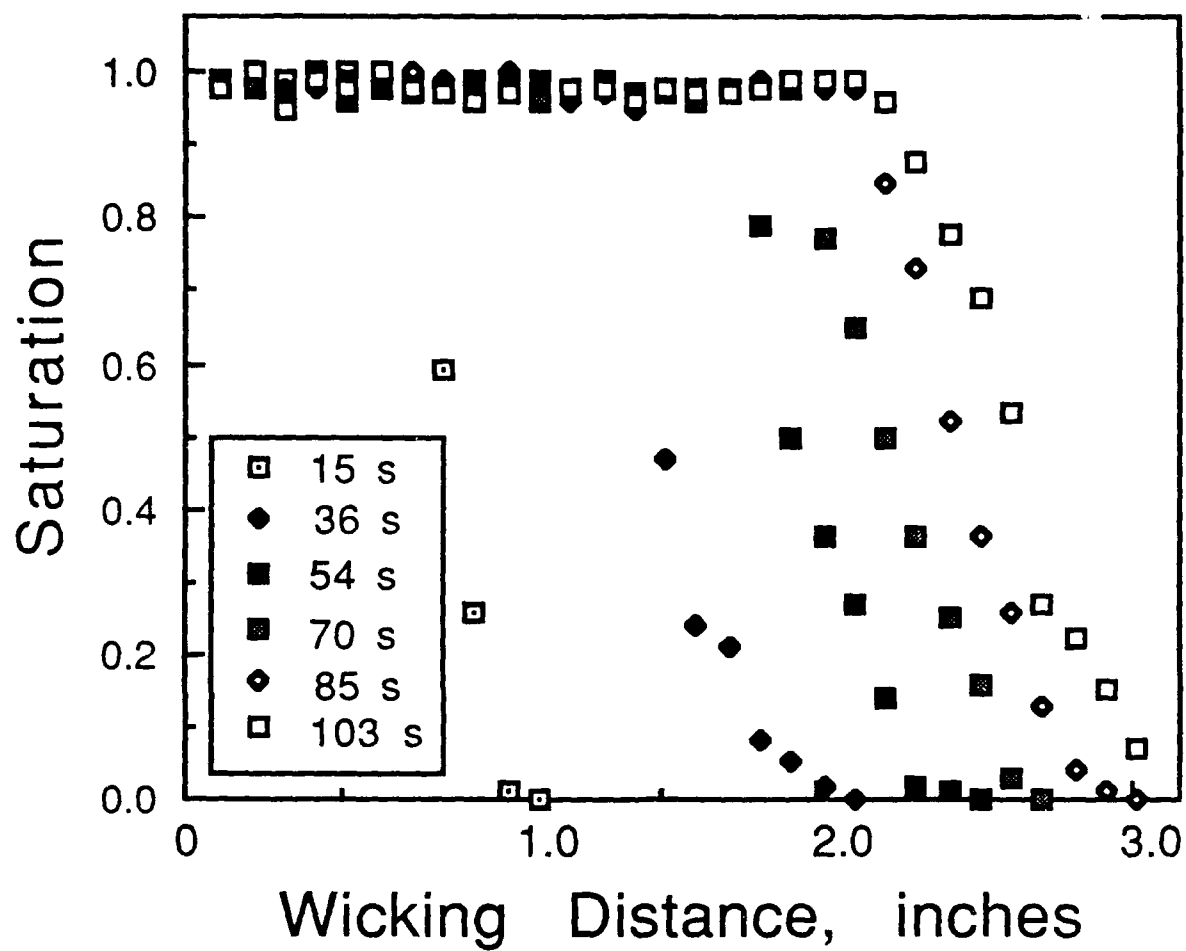


Figure 9 Transient Saturation Distribution, HC7-85 Wick

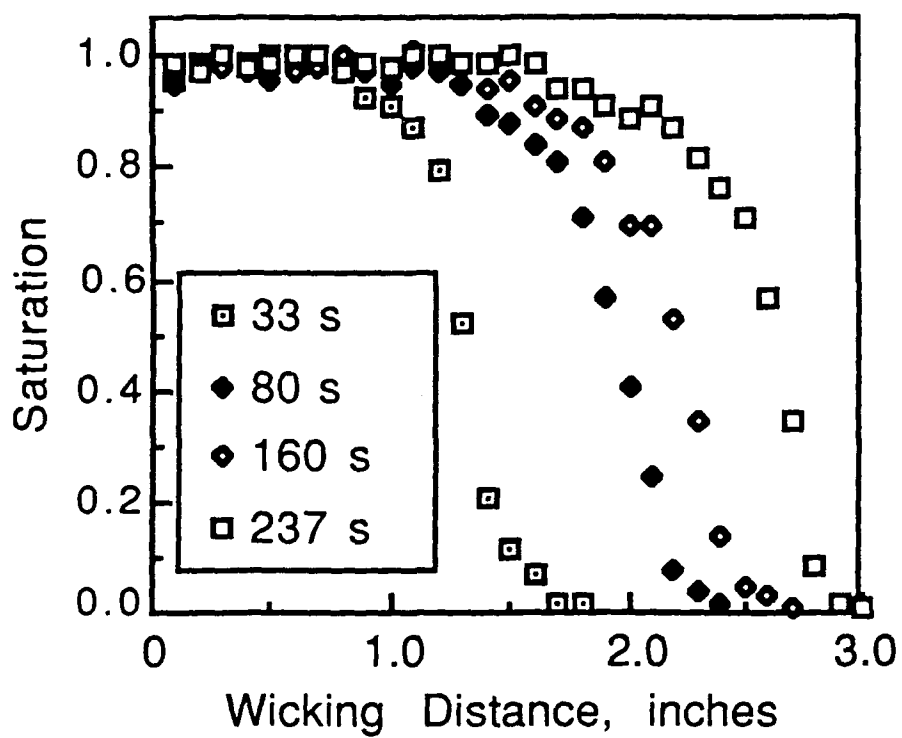


Figure 10 Transient Saturation Distribution, HC7-51 Wick

copper screen wicks. Both show a rapid rise to near equilibrium, followed by a very slow creeping flow.

5.5 DIMENSIONLESS CAPILLARY PRESSURE

The current steady-state data for the four different wick materials of Table 1 are shown in Figure 11. These values have been nondimensionalized using the Leverett function [4]

$$P^* = (P_c/\sigma)\sqrt{K/\epsilon}, \quad (5.5.1)$$

where P_c is the capillary pressure, σ the surface tension, K is the permeability and ϵ the porosity. The permeability was calculated based on the Blake-Kozeny equation [11]:

$$K = \frac{\epsilon^3 d^2}{122(1-\epsilon)^2} \quad (5.5.2)$$

where ϵ is the porosity and d the filament diameter. The porosity is based on the equation of Marcus [11]:

$$\epsilon = 1 - \frac{\pi C N d}{4} \quad (5.5.3)$$

where N is the mesh number and the "crimping factor" C is taken to be 1.05 because the wick is tightly pressed between the plates. Values of full permeability and porosity calculated using Eqns. (5.5.2) and (5.5.3) are given in Table 1.

Further data for a metal felt wick [7] and for clean sands [4] are compared with the present data in Figure 12. The good agreement for saturations between 0.1 and 0.9 is surprising, given both the differences in geometry of the porous materials and the additional uncertainty introduced by using Eqns. (5.5.2) and (5.5.3). A curve fit of the present data (for screen wicks) for saturations less than 0.9 is also shown in Figure 11. This curve fit was used in the calculation of relative permeabilities in the following section.

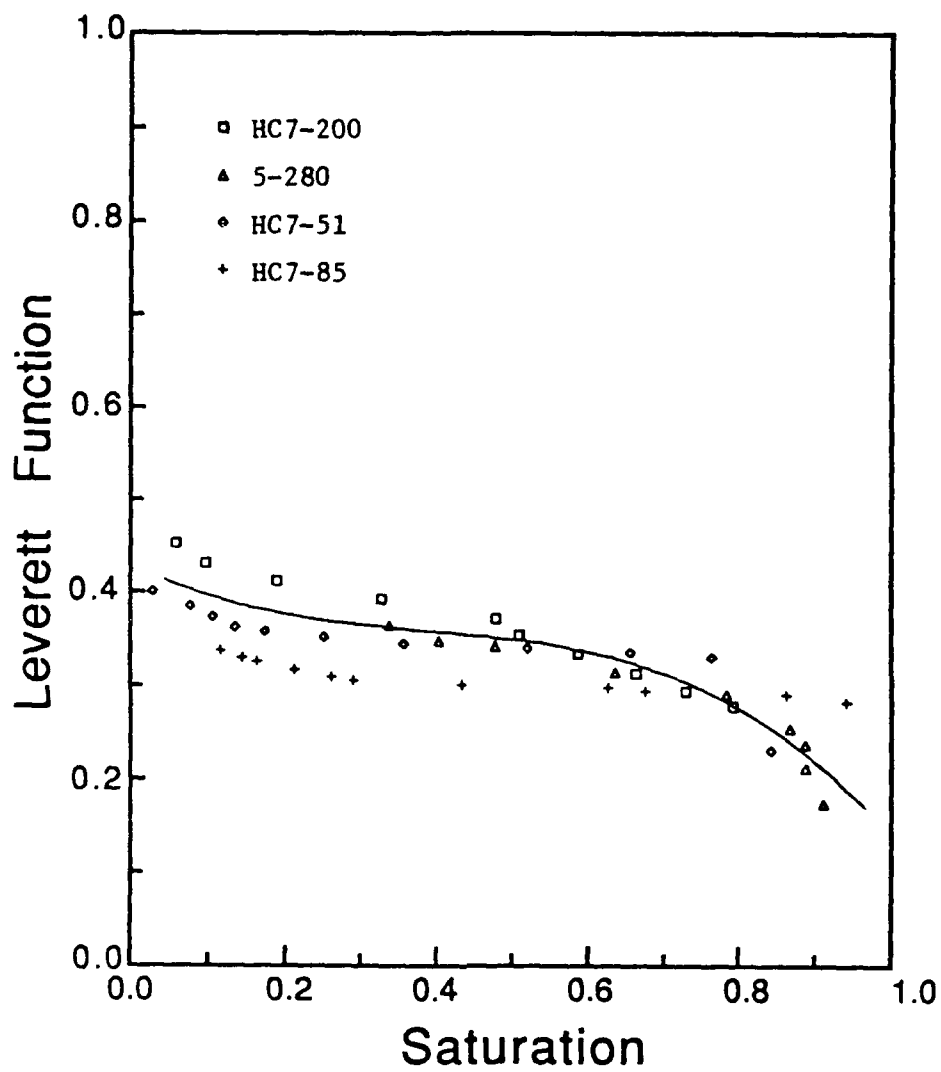


Figure 11 Dimensionless Capillary Pressure vs Saturation

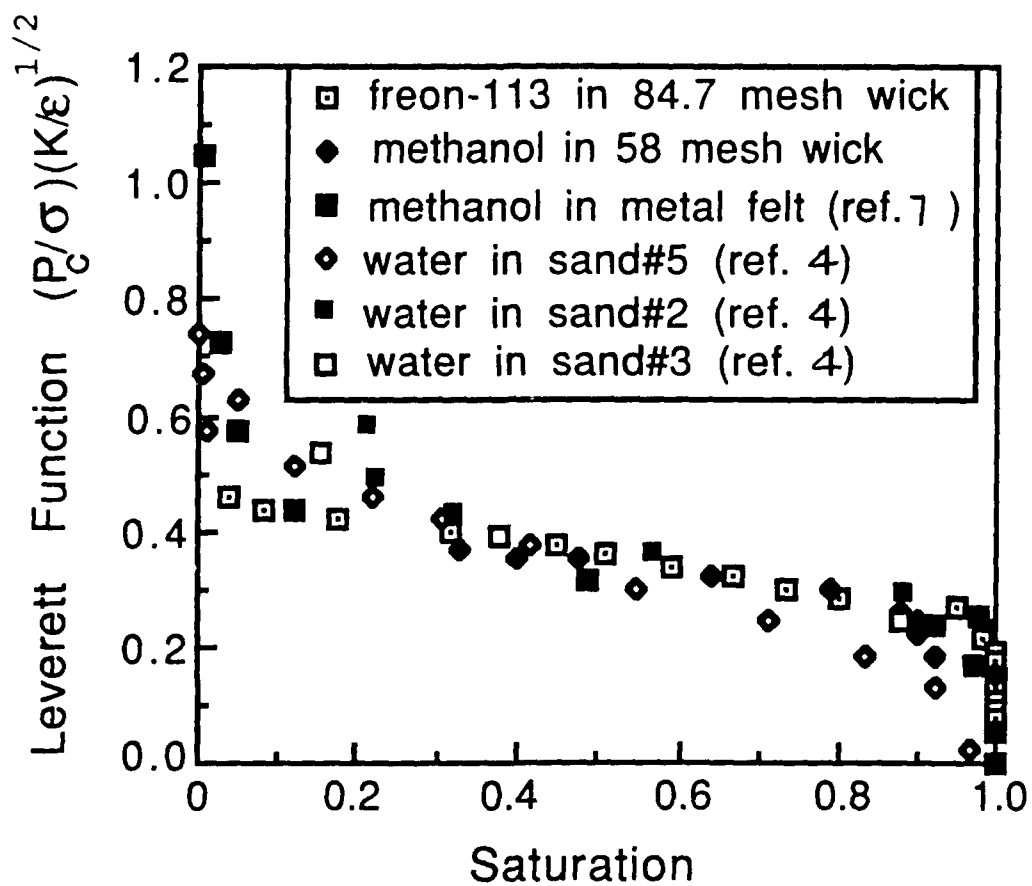


Figure 12 Leverett Function

5.6 GRAPHITE WICK MATERIAL

Samples of a porous graphite material have been obtained from Goodrich and Union Carbide Corps. and tested. The imaging of liquid (methanol, Freon-113) in these samples has been very successful, due to the low x-ray attenuation of carbon. The nondimensional capillary pressure is plotted versus saturation in Figure 13 for one of the graphite samples. This sample is designated PG-60 by Union Carbide, who supplied values of the porosity and full permeability as 0.48 and $5 \times 10^{-12} \text{ m}^2$, respectively. These capillary pressure data were obtained in a steady-state test with methanol (undoped) as the working fluid. X-ray energy was set at 14 kV. Included for comparison are data from [4] for sand and present data for a polyester mesh. The capillary pressure curve for the porous graphite material has the same shape as the mesh wicks, but falls somewhat lower. It is felt that the different final wicking heights are caused by a difference in the pore geometry, specifically the degree of interconnection of the pores.

Although these materials are markedly different in structure from the standard mesh wicks, they will be of value in verifying the liquid flow model. These samples have the advantage of being mechanically rigid. This fact makes them more desirable for testing in the actual heat pipe. In the heat pipe it is necessary to maintain good contact between the wall and wick. With the polyester mesh wicks, this may be difficult due to their highly flexible nature. The rigid porous graphite samples can be machined into a rectangular shape and pressed tightly against the beryllium wall of the heat pipe. The samples tested to date all have a porosity of 48 percent, which is relatively low compared to most heat pipe wick materials. Some samples with much higher porosity have been ordered from Oak Ridge National Laboratory.

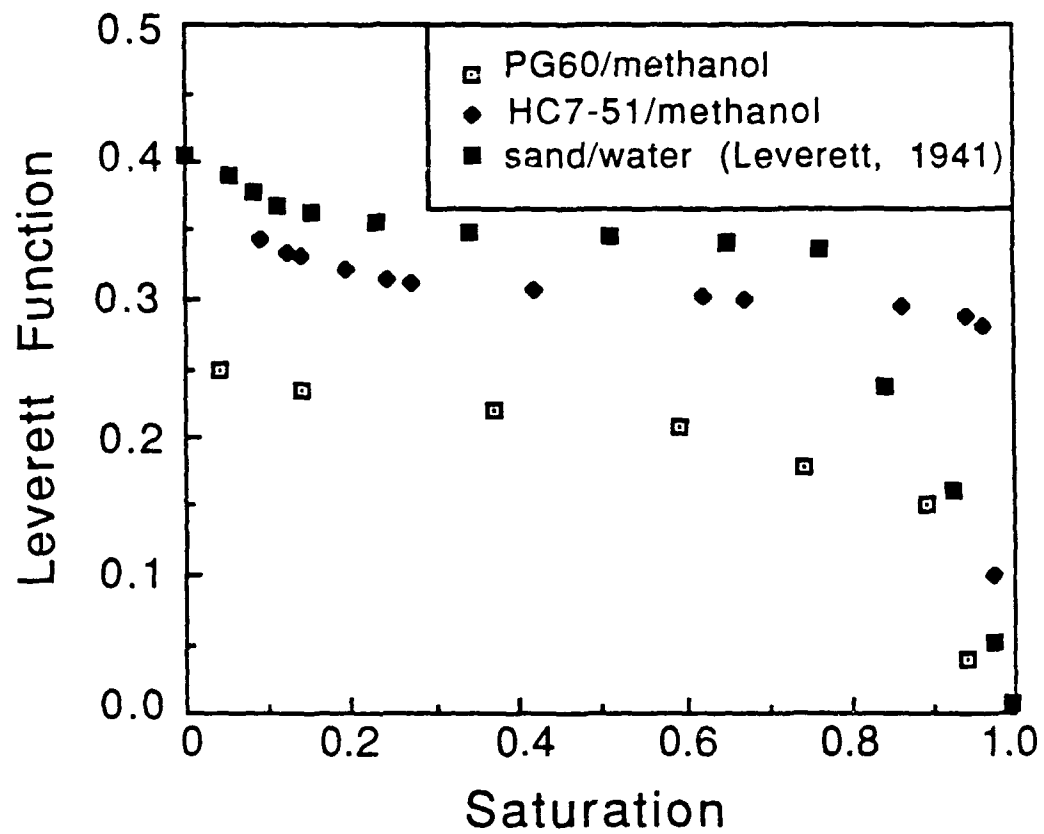


Figure 13 Leverett Function with Graphite Wick

VI. DETERMINATION OF RELATIVE PERMEABILITY

Relative permeability values have been obtained from the transient wicking rise tests. Experiments have also been performed to measure the relative permeability directly in a steady-state flow experiment. This experiment involves simultaneous measurement of the pressure and saturation distributions and mass flow rate in a wick with an induced capillary pressure gradient.

6.1 THEORY OF RELATIVE PERMEABILITY

Permeability of a porous medium, defined by Darcy Law, is generally measured with a single phase fluid occupying the medium. This value is referred to here as the full permeability. When a porous material is occupied by more than one phase, the permeability decreases. In this case, the movement of the phases are modeled separately, and a relative permeability is defined for each phase. This relative permeability is a function of the volume fraction of each phase present in the voids. When only a wetting and nonwetting phase are present, as in a heat pipe, the volume fraction is characterized by the saturation. The relative permeability to either phase has a value between 0 and 1. The effective permeability to each particular phase is the product of the relative permeability to that phase and the full permeability.

6.2 DETERMINATION OF RELATIVE PERMEABILITY FROM TRANSIENT WICKING TEST

Data for transient saturation distributions given in Figures 7 to 10 were used to calculate relative permeabilities. In order to obtain the relative permeability from the data, Darcy law is used:

$$U(x) = - \frac{K_r(S)K}{\mu} \frac{dP}{dx} . \quad (6.2.1)$$

Here U is the superficial flow velocity, μ is liquid viscosity and x is distance along the wick in the direction of the flow, measured from the

reservoir. In the transient case P is not known directly, so it is written in terms of saturation S ,

$$P = P_0 - (P_c - \rho g x \sin \theta), \quad (6.2.2)$$

$$\frac{dP}{dx} = \rho g \sin \theta - \frac{dP_c}{dS} \frac{dS}{dx}. \quad (6.2.3)$$

Here P_0 is the liquid pressure (atmospheric) at the level of the reservoir. The function dP_c/dS is taken to be a property of the wick structure and is obtained from the equilibrium data (Figure 11). The saturation gradient and flow velocity are obtained from the transient saturation distributions as follows. Let $S_1(x)$ and $S_2(x)$ represent the saturation distributions with distance at times $t=t_1$ and $t=t_2$ respectively, where $t_2-t_1=\Delta t$. The saturation gradient used in the calculation of relative permeability is:

$$\left. \frac{dS}{dx} \right|_{x_0} = \frac{1}{2} \left\{ \left. \frac{dS_2}{dx} \right|_{x_0} + \left. \frac{dS_1}{dx} \right|_{x_0} \right\} \quad (6.2.4)$$

The flow velocity is given by:

$$U(x_0) = \frac{\int_{x_0}^{x_\infty} S_2(x) dx - \int_{x_0}^{x_\infty} S_1(x) dx}{\Delta t / \epsilon} \quad (6.2.5)$$

where x_∞ is the position at which $S=0$ and the saturation of interest is $S(x_0) = \{S_2(x_0) + S_1(x_0)\}/2$. Reynolds numbers based on the velocity calculated from the data and the pore opening are of the order of 0.1. Darcy law is generally assumed valid in this regime. The momentum boundary layer formed near the solid wall is of the order of $\sqrt{K/\epsilon}$ in Darcy flow [12]. For the materials of interest, this value is of the order of 10 μm or less ($\sim 0.1\%$ of the wick thickness). Because of this, the number of layers is assumed to have a negligible effect on the flow properties.

The relative permeability is given in Figure 14 as a function of saturation for the four different meshes. The significant amount of scatter in the data is to be expected because of the uncertainty associated with

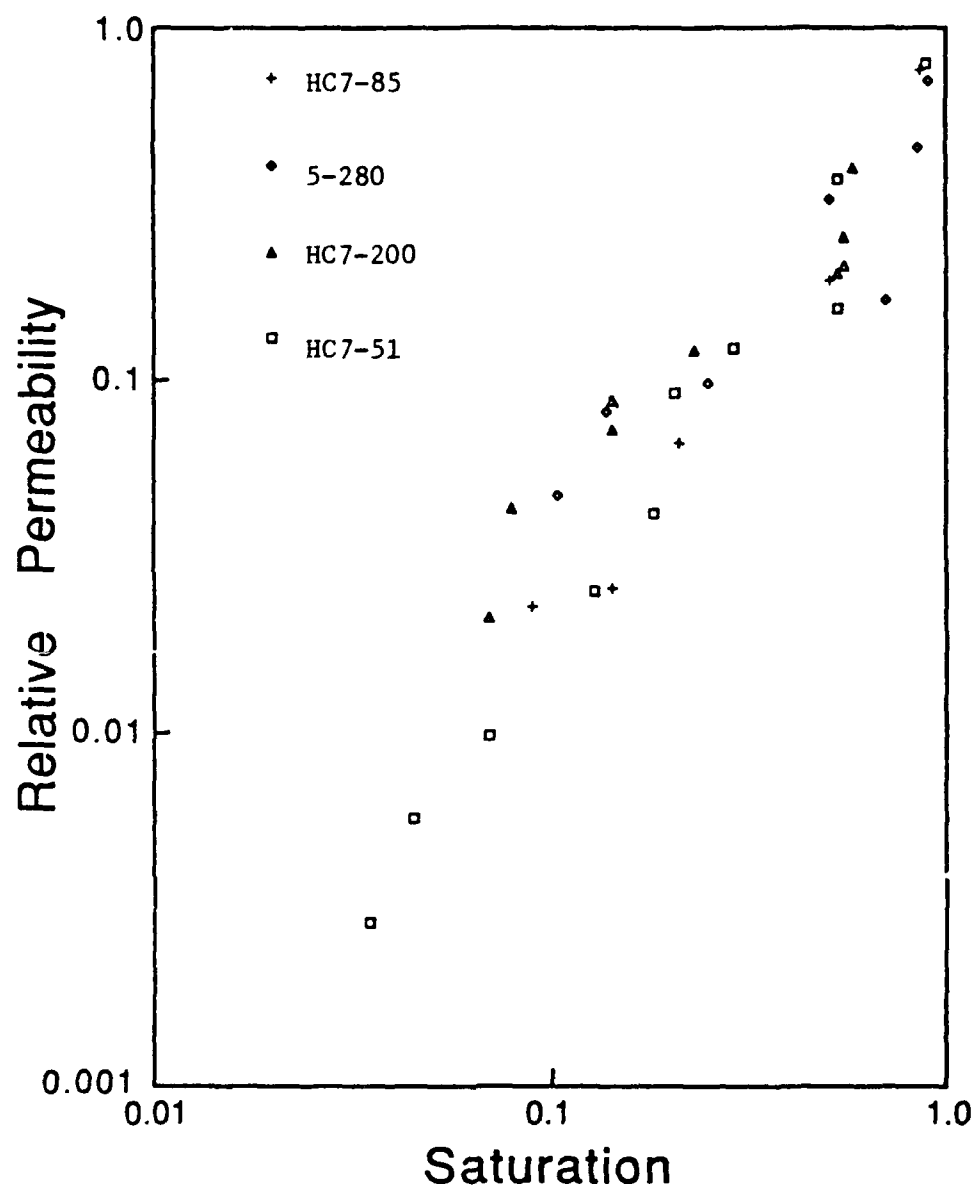


Figure 14 Relative Permeability vs Saturation

extracting gradients from the data. The present data are best fit using the equation:

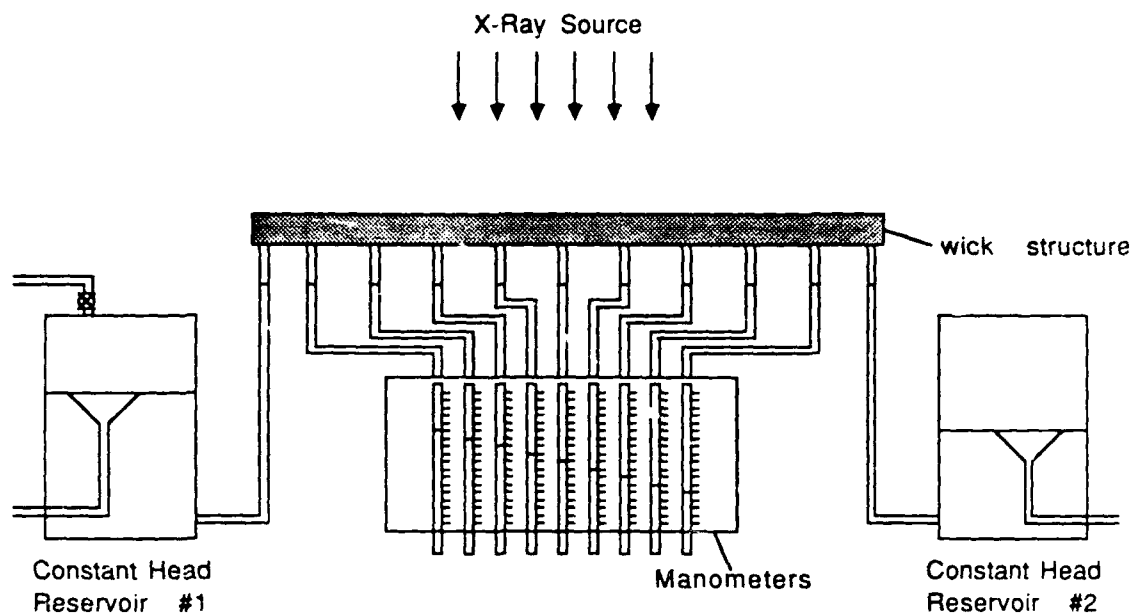
$$K_r = S^{1.65} . \quad (6.2.6)$$

6.3 RELATIVE PERMEABILITY EXPERIMENTS

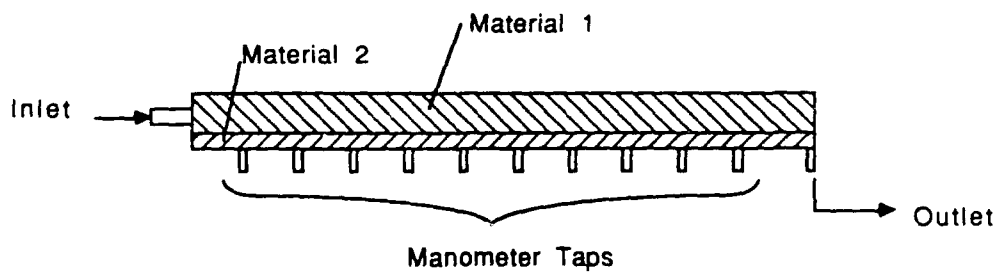
A new apparatus was designed and fabricated specifically to obtain direct measurements of the relative permeability in a partially saturated screen wick. These measurements are necessary to verify the validity of the transient wicking rise technique. The new apparatus is designed to allow a larger pressure gradient (greater than the maximum capillary head) across the wick structure without depriving the manometer or outlet taps.

The design of the new apparatus is shown in Figure 15. Two different wick materials are used to form the wick structure. The two wick design is similar to that used by Eninger [7] to measure nonlinear pressure gradients in porous metal fiber wicks. The upper wick is of larger pore size than the lower wick. As such, it develops a lower capillary pressure. It also has a higher full permeability. The upper wick also is larger in cross sectional area. When an axial pressure gradient is applied across the composite structure, it is the same in both wick materials provided the liquid wets both materials. The flow occurs mainly in the upper wick because of the higher permeability and larger flow area. As the pressure in the outlet portion of the wick structure is reduced, the upper wick will become partially saturated first, because it cannot support the capillary head. The lower wick remains fully saturated because of its higher capillary pumping. Since the manometer taps and flow outlet originate in the lower wick, these remain wetted. Thus the pressure distribution in the partially saturated upper wick may be measured provided the lower wick remains fully saturated.

The total mass flow rate through the composite structure is measured. When both wicks are fully saturated, over 95 percent of the flow is through the upper wick. But as the upper wick desaturates, its permeability becomes lower, and more flow occurs in the lower wick. The relative permeability of the upper wick is given by:



Schematic of Relative Permeability Test



Detail of Wick Structure

Figure 15 New Apparatus for Measuring Relative Permeability

$$K_{lr} = \frac{\frac{\dot{m} \nu}{dP/dx} - K_2 A_2}{K_1 A_1} \quad (6.3.1)$$

where the correction accounts for the flow through the fully saturated lower wick of known full permeability.

Saturation measurements will be obtained as in the previous experiments by radiographing the composite wick structure. The procedure will be slightly more complicated than previous arrangements because of the composite structure. Instead of radiographing only a dry wick structure as a baseline, the baseline optical density must include the effects of the dry upper wick and the fully saturated lower wick, as well as the wall material.

6.4 PRELIMINARY RESULTS

Initial tests were conducted to verify that the flow was occurring mainly in the upper wick (material #1) for the fully saturated case. For these tests, the upper wick (material #1) was 5-280, the lower wick (material #2) was 7-51 and both water and methanol were used as working fluids. To ensure that the wick structure was fully saturated, the head in both reservoirs was maintained at a level well above the actual level of the wick structure and gas bubbles were bled from all taps. Values of the full permeability calculated from these tests were within 20 percent of the predicted value in Table I.

Further testing of the apparatus was conducted using the same wicks and Freon-113 as the test fluid. For the earliest tests, the x rays were taken at 15 kV. This energy level gives the best contrast in the radiographs of Freon. Exposure time was set based on the dry apparatus so that the radiographs had the highest measurable optical density (5D). However, with these exposure parameters, the working fluid blocked nearly all of the x rays, resulting in insufficient optical intensity on the radiographs. Several different pressure distributions and resulting mass flow rates were measured nonetheless. To allow for accurate saturation measurements, we decided to increase the x-ray energy and reduce the exposure time. Several tests have been run with the new

exposure parameters and the radiographs are of sufficient optical density to obtain saturation measurements. The saturation measurements are incomplete as of the date of this report. Still required are the baseline radiographs of the wall, dry wick material #1 and fully saturated material #2.

VI. CONCLUSIONS AND RECOMMENDATIONS

The equilibrium data in Figure 11 show the validity of the dimensionless scaling proposed by Leverett [4] for screen wick materials. The data for different fluids and different types of wick structures correlate well. The transient wicking data agree qualitatively with the earlier results of Beam [10] which show a rapid initial climb toward the final equilibrium wicking height. Relative permeability values have been obtained from transient wicking rise curves. These values have a good deal of uncertainty due to the complexity of the data reduction calculations. However, the experimental procedure is much less complex than the usual methods for measurement of relative permeabilities. Currently, the relative permeability values are being verified by direct simultaneous measurement of saturation and pressure distributions in a flow in a partially saturated wick. The experimental apparatus being used is similar to that of Eninger [7] with the addition of the saturation measurement utilizing X-ray radiography.

REFERENCES

1. Udell, K.S., "Heat Transfer in Porous Media Heated from Above with Evaporation, Condensation and Capillary Effects," J. Heat Transfer, Vol. 105, No. 3, pp. 485-492, 1983.
2. Udell, K.S., "Heat Transfer in Porous Media Considering Phase Change and Capillarity - the Heat Pipe Effect," Int. J. Heat Mass Transfer, Vol. 28, No. 2, pp. 485-495, 1985.
3. Fitch, J.S. and K.S. Udell, "Limits of Multiphase Heat and Mass Transfer in Porous Media," ASME Paper 86-HT-33, AIAA/ASME 4th Joint Thermophysics and Heat Transfer Conf., Boston, MA, 1986.
4. Leverett, M.C., "Capillary Behavior in Porous Solids," Trans. AIME, Vol. 142, pp. 152-169, 1941.
5. Scheidegger, A.E., The Physics of Flow Through Porous Media, MacMillan Co., New York, 1957.
6. Ambrose, J.H., L.C. Chow and J.E. Beam, "Measurement of Liquid Flow in Heat Pipe Wicks," AIAA Paper 87-1647, 22nd AIAA Thermophysics Conf., Honolulu, HI, 1987.
7. Eninger, J.E., "Capillary Flow Through Heat-Pipe Wicks," Progress in Astronautics and Aeronautics, Vol. 49, Ed. A.M. Smith, 1976.
8. Brown, H.W., "Capillary Pressure Investigations," Trans. AIME, Vol. 192, pp. 67-74, 1951.
9. Shibayama, S. and S. Morooka, "Study on a Heat Pipe," Int. J. Heat and Mass Transfer, Vol. 23, pp. 1003-1013, 1980.
10. Beam, J.E., Unsteady Heat Transfer in Heat Pipes, PhD Dissertation, School of Engineering, University of Dayton, Dayton, OH, 1985.

11. Chi, S.W., Heat Pipe Theory and Practice, McGraw-Hill, 1976.
12. Vafai, K. and C.L. Tien, "Boundary and Inertia Effects on Flow and Heat Transfer in Porous Media," Int. J. Heat and Mass Transfer, Vol. 24, pp. 195-203, 1981.